Research

Author for correspondence:
Chad M. Eliason
e-mail: cme16@zips.uakron.edu

Royal Society **Publishing**
Informing the science of the future

How hollow melanosomes affect iridescent colour production in birds

Chad M. Eliason[1], Pierre-Paul Bitton[2] and Matthew D. Shawkey[1]

[1]Department of Biology and Integrated Bioscience Program, The University of Akron, Akron, OH, USA
[2]Department of Biological Sciences, University of Windsor, Windsor, Ontario, Canada

Developmental constraints and trade-offs can limit diversity, but organisms have repeatedly evolved morphological innovations that overcome these limits by expanding the range and functionality of traits. Iridescent colours in birds are commonly produced by melanin-containing organelles (melanosomes) organized into nanostructured arrays within feather barbules. Variation in array type (e.g. multilayers and photonic crystals, PCs) is known to have remarkable effects on plumage colour, but the optical consequences of variation in melanosome shape remain poorly understood. Here, we used a combination of spectrophotometric, experimental and theoretical methods to test how melanosome hollowness—a morphological innovation largely restricted to birds—affects feather colour. Optical analyses of hexagonal close-packed arrays of hollow melanosomes in two species, wild turkeys (*Meleagris gallopavo*) and violet-backed starlings (*Cinnyricinclus leucogaster*), indicated that they function as two-dimensional PCs. Incorporation of a larger dataset and optical modelling showed that, compared with solid melanosomes, hollow melanosomes allow birds to produce distinct colours with the same energetically favourable, close-packed configurations. These data suggest that a morphological novelty has, at least in part, allowed birds to achieve their vast morphological and colour diversity.

1. Introduction

Evolutionary diversification of morphological traits can be constrained by factors such as trade-offs (e.g. between song frequency and trill rate in Darwin's finches [1]) and developmental processes (e.g. close packing of cells that limit branching patterns in plants [2]). However, innovations in form or change in the form–function relationship may remove these constraints and allow for enhanced diversity [3]. Colourful plumage patches in birds are complex, and diverse multi-component traits [4] that can be used to attract mates, avoid predators, or recognize conspecifics [5,6]. Feather colours are produced by light absorption by pigments and/or coherent light scattering by nanoscale arrangements of feather materials (keratin, melanin and air) that periodically vary in refractive index [7]. The latter (structural colours) are frequently produced by melanin-containing organelles (melanosomes) that likely self-assemble during development [8] to form thermodynamically stable, ordered structures such as hexagonal close-packed arrays [9]. However, for solid melanosomes, the observed variations of this hexagonal configuration, and hence the properties of colours they produce, are low relative to what is theoretically possible [10]. Achieving brighter or more saturated colours would require either (i) enhancing the refractive index contrast or (ii) increasing the relative amount of low refractive index material (in this case, keratin) by adding space between melanosomes, potentially decreasing order [11] and therefore thermodynamic stability during development.

Hollow melanosomes are morphological innovations that have likely evolved independently in at least seven avian families, including some that are notable for both the diversity and conspicuousness of their iridescent feathers (e.g. Galliformes) [9,12,13]. The replacement of melanin with air in the core of hollow melanosomes has potentially important optical consequences, as it introduces both a low refractive index material (air) that can be tuned

independent of melanosome spacing, and a sharp refractive index contrast along the direction perpendicular to the melanosome axis. However, these consequences have never been fully quantified, limiting our understanding of their potential evolutionary significance. In this study, we used both theoretical modelling and empirical data to examine the mechanisms of colour production by hollow melanosomes in two focal species, the wild turkey (*Meleagris gallopavo*) and the violet-backed starling (*Cinnyricinclus leucogaster*), and incorporated survey data from additional species to compare the colours produced by both hollow and solid hexagonal close-packed melanosomes.

2. Methods

(a) Experimental overview
The iridescent structures of birds, found in the barbules of feathers, are physically best described as photonic crystals (PCs), or nanostructures composed of materials with different refractive indices occurring at regular intervals. These materials can be ordered in one-, two- or three-dimensions [7]. Depending on the organization of and distance between repeating materials, certain wavelengths of light will pass through the structure, whereas others will not. To characterize the PCs created by hollow melanosomes, we sampled iridescent feathers from two focal species with hexagonal close-packed hollow melanosomes of different sizes [2] and quantified their morphologies using transmission electron microscopy. We then determined feather colour and tested hypotheses on the nature of the nanostructure by measuring reflectance as a function of angle and light polarization. To understand the colour-producing mechanism, we computed theoretical spectra based on the observed morphologies and compared the results with the empirical spectra. Using this optical model, we simulated the range of colours achievable with both solid and hollow melanosomes and plotted morphological and colour data from a broader set of taxa in this theoretical colourspace. Detailed methodology is available in the electronic supplementary material.

(b) Morphological analysis
To examine their nanostructure, we imaged barbule cross sections with transmission electron microscopy (TEM) following Shawkey *et al.* [14]. To further confirm nanostructural details, we examined longitudinal sections of unprepared barbules with scanning electron microscopy (SEM). From the TEM images, we measured the following parameters known to be significant to colour production on two to four barbule regions per individual per species: air space radius in the interior of melanosomes (r_{air}), melanosome radius (r_{mel}), thickness of the keratin cortex taken at 10 locations along the barbule edge and number of melanosome layers perpendicular to the feather surface (see electronic supplementary material, figure S1 for schematic). The wavelength of peak reflectance (hue) in PCs is largely determined by the spacing between particle centres (lattice constant a), whereas brightness is a function of the refractive index contrast (n_{high}/n_{low}) and relative proportion of low-index material (openness) [15]. In our case, the lattice constant is the melanosome diameter, the refractive index contrast is $n_{mel}/n_{air} = 2$, and openness is the proportional amount of air within melanosomes ($l^* = r_{air}/r_{mel}$). To compare the properties of hexagonal arrays of hollow and solid melanosomes, we calculated these variables from published data (see electronic supplementary material, table S1 for species and references) along with an additional openness metric for solid melanosomes ($w^* = w/a$, where w is the distance between adjacent melanosomes).

(c) Spectral analysis
Two-dimensional PCs differ from one-dimensional PCs in their ability to scatter light depending on polarization and propagation direction. For example, because one-dimensional PCs have a uniform refractive index parallel to the surface they can only produce colour specularly (with the observer angle equal to the incident angle) and the reflected colour at normal incidence (0°) is unpolarized [16]. By contrast, two-dimensional PCs can diffract light (causing visible colour when the observer angles differ from the incident angle), and the reflected colour at normal incidence is polarized [16]. To examine the optical properties of these nanostructures, and to test whether they are consistent with those of two-dimensional PCs, we determined backscattered, diffuse, and specular reflectance at different polarizations. From the resulting curves, we calculated brightness (peak height, R_{max}), hue (peak location, $\lambda_{R_{max}}$) [17] and saturation (full width of peak at half maximum) using the R package PAVO v. 0.1–2 [18].

(d) Refractive index-matching experiments
In both species, we observed a continuous layer of keratin (cortex) overlying melanosomes (figure 1b,d). To test whether interference from this layer produces the observed colours, we minimized its effect by performing a refractive index-matching experiment [10].

(e) Optical modelling
We used two modelling approaches to understand how light interacts with feather morphology. First, we used the plane-wave expansion method implemented in the program MPB [19] to build photonic band gap models and thus predict reflected colour as a function of incident angle (axes in a band structure diagram). Second, to make detailed comparisons with empirical reflectance spectra, we used the finite-difference time-domain method implemented in MIT electromagnetic equation propagation [20] to predict reflectance spectra for different polarizations and incident angles.

(f) Colourspace analysis
We calculated the range of colours that could theoretically be produced by variation in the morphology of two-dimensional hexagonal PCs composed of either solid or hollow melanosomes and compared the distributions of empirical morphologies and colours for each melanosome type in this theoretical colourspace using published data (see electronic supplementary material, table S1).

3. Results

(a) Morphological analysis
Iridescent feather barbules from both focal species contained a well-ordered hexagonal lattice of close-packed, rod-shaped hollow melanosomes beneath a keratin cortex (figure 1b,d and electronic supplementary material, figure S2). Turkeys had larger melanosome diameter than starlings, but the proportional amount of air within melanosomes (openness) was similar (see electronic supplementary material, table S1). Turkeys also had an additional layer of melanosomes compared with starlings (4.7 ± 0.1 versus 3.5 ± 0.1) and a much thicker keratin cortex (1075.5 ± 4.9 versus 114.5 ± 5.8 nm). Melanosome size estimates based on angle-resolved measurements matched the TEM values fairly well (see electronic supplementary material, appendix S5 and table S2). Fast-Fourier transforms (FFTs) of isolated regions of melanosomes indicated hexagonal periodicity
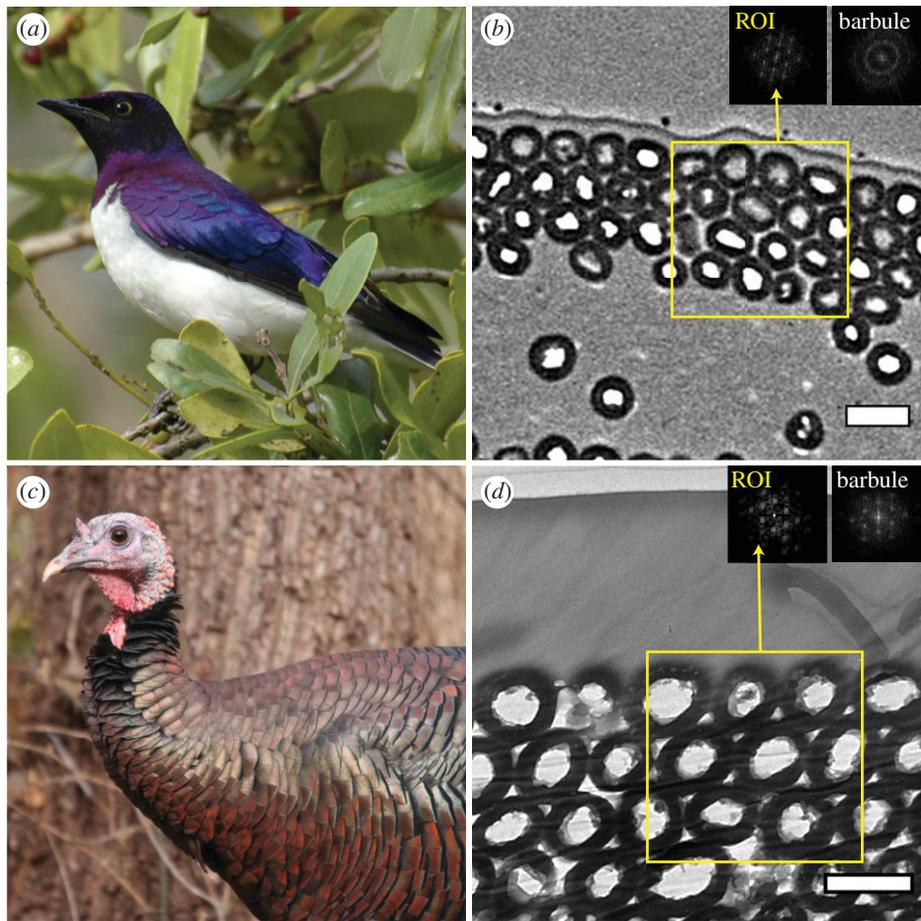
Figure 1. Hollow melanosome morphology in iridescent feathers. Images show representative individuals and corresponding TEM images of feather barbule cross sections in violet-backed starlings (*a,b*) and wild turkeys (*c,d*). Insets in (*b*) and (*d*) are fast-Fourier transforms (FFTs) of regions of interest (yellow boxes) and upper barbule surface (portion including top stack of melanosome layers). Scale bars, 500 nm. Photo credits: (*a*) Ken Clifton, (*c*) anonymous.

for both species (figure 1*b,d*, left insets). However, FFTs of the whole-barbule surface (the complete nanostructure) differed. Because starling barbules are curved, the orientation of isolated regions of melanosomes varies along the barbule surface, resulting in an FFT pattern of concentric rings suggesting a loss of hexagonal periodicity (figure 1*b*, right inset). By contrast, turkeys have flatter barbules, and the whole-barbule FFT again showed hexagonal periodicity (figure 1*d*, right inset).

(b) Spectral analysis

Starling feather reflectance spectra at near-normal incidence showed a primary peak at around 800 nm and a secondary peak at 400 nm (figure 2*a*). The curves substantially differed depending on the incident light polarization. Specifically, the main peak was brighter and blue-shifted for TE- relative to TM-polarized light (figure 2*a*). Reflectance spectra of turkey feathers at near-normal incidence (10°) showed a primary peak extending into near-infrared wavelengths and a secondary 'double peak' centred at around 500 nm (figure 2*b*). Similar to starlings, the shape of the reflectance curves for wild turkeys differed with polarization: for TE-polarized light, the green peak decreased in reflectance and the infrared peak became much broader and taller compared with that for TM-polarized light (figure 2*b*). Backscattering reflectance of starling feathers revealed that the locations of both peaks remained largely invariant with increasing tilt angle and reflectance decreased only slightly, with the violet colour remaining visible at tilts above 60° (figure 2*c*). For turkey feathers, as tilt

angle increased, there was an abrupt shift in colour as a new peak appeared between 650 and 700 nm (figure 2*d*). This red peak reached a maximum reflectance at a feather tilt of approximately 45° and was visible only when the viewing angle was perpendicular to the feather barbules. Diffuse measurements indicated that starling colour remained visible over a wider range of diffuse angles than turkeys (see electronic supplementary material, figure S3*a*). Turkey feathers additionally showed a faint but discrete peak shift from 520 to roughly 600 nm (see electronic supplementary material, figure S3*b*), consistent with the colour change observed in backscattering measurements.

(c) Refractive index-matching experiments

For starlings, when feathers were immersed in oil, both peaks shifted to slightly shorter wavelengths and the main peak broadened (see electronic supplementary material, figure S4*a*). For turkeys, the double reflectance peak near 500 nm diminished (i.e. became a single peak; electronic supplementary material, figure S4*b*). To test whether this latter effect is produced by thin-film interference by the keratin cortex, we determined the wavelengths of two consecutive local reflectance maxima and used a published equation (equations (6–9) in Ohring [21]) to predict film thickness given $n_{ker} = 1.56$. We inferred a cortex thickness of 1098 nm, in good agreement with that measured directly from TEM images (1076 nm). We could not perform this calculation in violet-backed starlings because the cortex was too thin (115 nm) to produce multiple reflectance peaks in visible wavelengths.
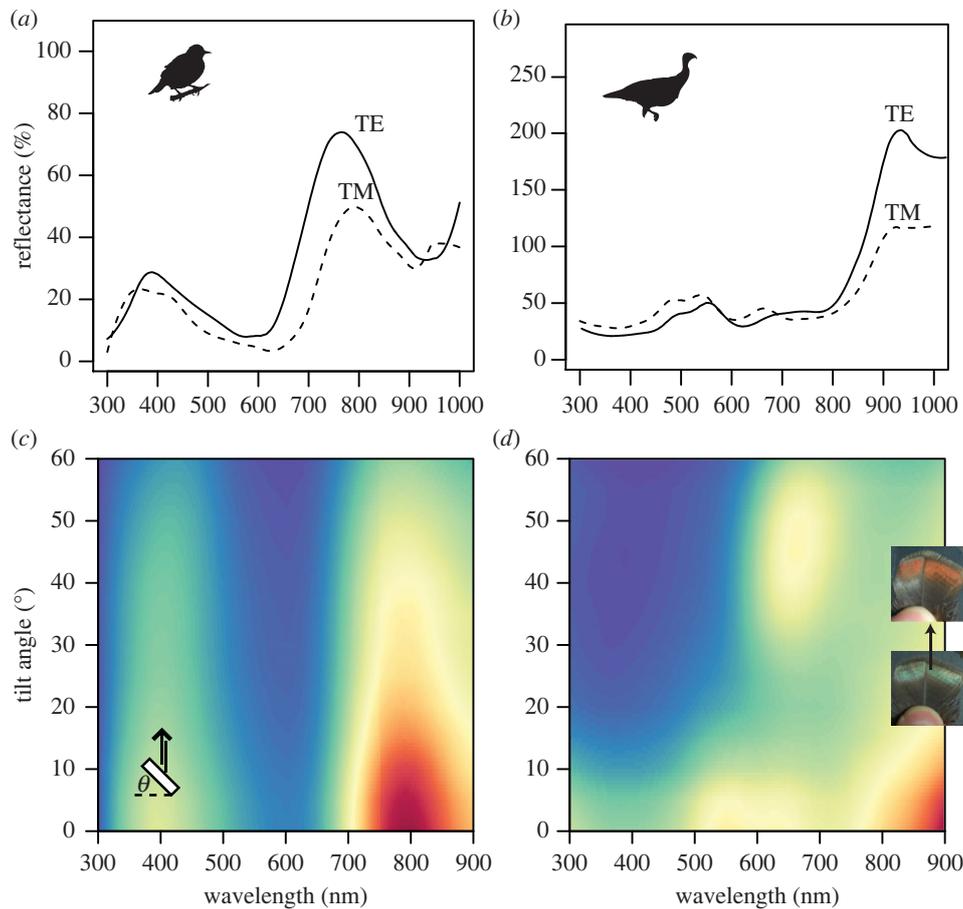
Figure 2. Effects of light polarization and feather tilt on reflectance of iridescent feathers. (*a,b*) Reflectance spectra of iridescent contour feathers of violet-backed starlings (*a*) and wild turkeys (*b*) for TE- (solid lines) and TM-polarized light (dashed lines) at near-normal incidence (10°; note different *y*-axis scales). (*c,d*) False colour maps show reflectance in arbitrary units (minimum, blue; maximum, red) versus wavelength and tilt angle in starlings (*c*) and turkeys (*d*). Schematic drawing in (*c*) illustrates feather barbule cross sections (white rectangle), incident and reflected light geometries (black arrows) and tilt angle *θ*. Outsets in (*d*) show a turkey feather at 0° (bottom) and approx. 45° tilt (top).

(d) Optical modelling

Optical simulations revealed a partial photonic band gap at normal incidence (along the *ΓM* direction) that was wider for TE- than TM-polarized light (see electronic supplementary material, figure S5). Additional partial band gaps opened up at multiples of this primary gap corresponding to higher-order Bragg reflections (shaded boxes around 400–500 nm in figure 3; note bold lines indicating light at normal incidence). Empirical reflectance curves at near-normal incidence (10°) matched the theoretical spectra calculated at the same angle moderately well, i.e. the predicted peak locations at normal incidence are about where expected from the empirical results (figure 3*a,b*). From the photonic band structure calculations, the reflectance peaks for both species occur about where first- and second-order Bragg diffraction is expected (shaded boxes in figure 3*a,b*). The colour change with feather tilt was explained well by the model (hue change approx. 120 nm versus 130 nm for the modelled and empirical results; figure 3*b*) and corresponded to reflection from melanosome rows tilted 30° from the feather surface. Additionally, our calculations of the empirical band structure from specular reflectance data matched the predicted results fairly well (see electronic supplementary material, figure S6 and appendix S6).

(e) Colourspace analysis

Simulated colours over a range of theoretical morphologies showed that hollow melanosomes have, on average, larger gap–midgap ratios than solid ones (figure 4*a*). Furthermore, the optimal configurations differed: for hollow melanosomes, the nanostructure with the largest gap–midgap ratio was close-packed (darkest grey line in figure 4*a*), but for solid melanosomes, the optimal nanostructure was non-close-packed. Empirical data showed that species with solid melanosomes had less open morphologies with smaller predicted gap–midgap ratios (figure 4*a*). By contrast, species with hollow melanosomes had more open morphologies with larger predicted gap–midgap ratios (figure 4*a*). Open structures produce reflectance spectra with broader reflectance peaks, leading to predictably brighter but less saturated colours than less open structures. The distribution of empirical colour data in colourspace showed that surveyed species with hollow melanosomes had broader reflectance peaks than those with solid melanosomes (figure 4*b*), but similar hue and brightness values.

4. Discussion

We demonstrate that the colour-producing mechanism in violet-backed starlings and wild turkeys is a two-dimensional PC consisting of hexagonal close-packed hollow melanosomes. Combined with optical simulations and survey data, our results suggest that hollow melanosomes allow birds to produce a broader range of colours with close-packed configurations than solid melanosomes.
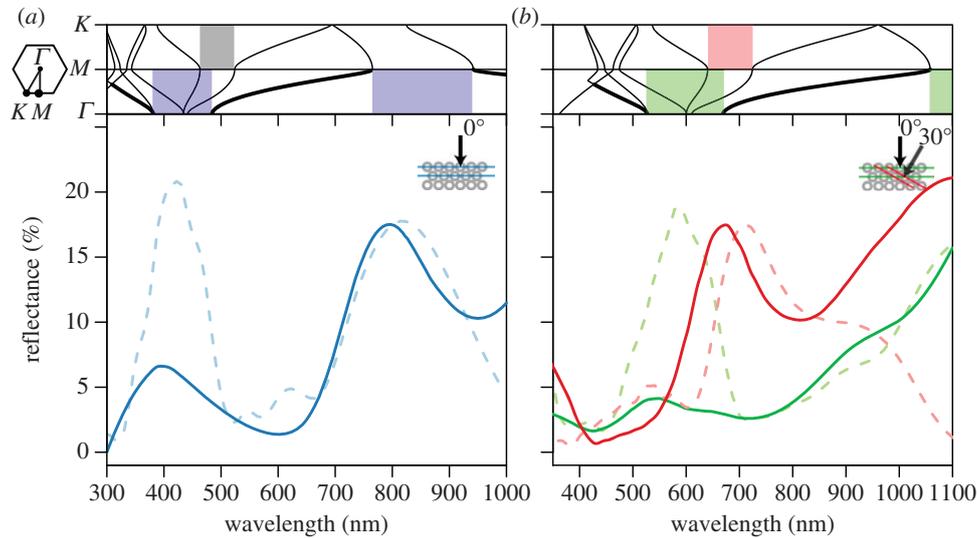
Figure 3. Calculated photonic band structure and match between predicted and empirical reflectance spectra for hollow close-packed melanosomes in violet-backed starlings (*a*) and wild turkeys (*b*). Upper portions of panels show angle of incident light versus wavelength for TE-polarized light (electric field perpendicular to melanosomes). Lines corresponding to normal incidence (0°) are bolded and shaded boxes depict partial photonic band gaps for rows of melanosomes illustrated in lower schematics. Outset illustrates first brillouin zone (hexagon) with high symmetry points (Γ, *M* and *K*) corresponding to different crystal planes. Lower parts of panels show empirical (continuous lines) and predicted reflectance (dashed lines) for starlings at near-normal (10°) incidence with no feather tilt (*a*) and turkeys, both with the feather flat (green lines) and at a tilt of roughly 45° (red lines, *b*), corresponding to an interior angle of approximately 30° after taking into account refraction by the keratin cortex following [22]. We did not observe discrete colour change with feather tilt in starlings, thus spectral data are not presented. Empirical spectra were smoothed to remove noise and adjusted to the FDTD results to permit easier comparison with modelled spectra. Parameters used in calculations were $r_{mel}/a = 0.5$, $l^* = 0.55$, $n_{mel} = 2$, $k_{mel} = 0.1$ and $n_{ker} = 1.56$.
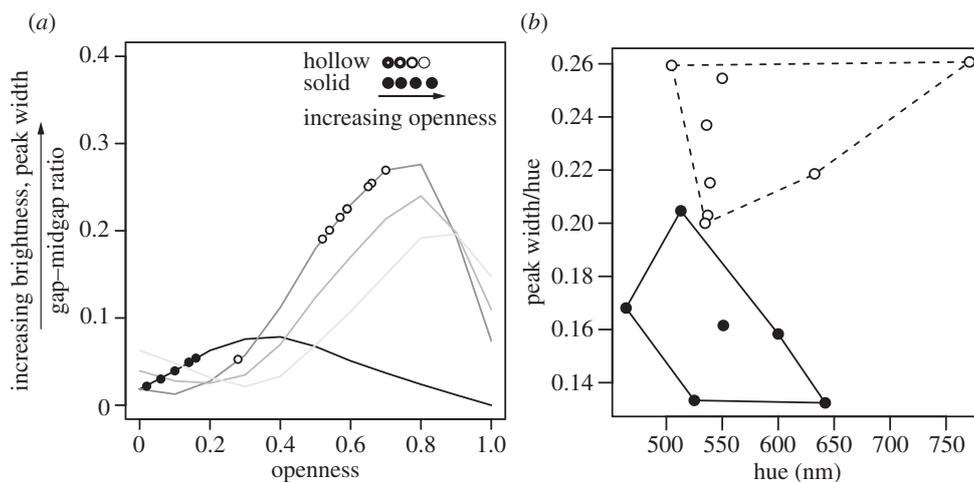

Figure 4. Theoretical and empirical colourspace diagrams for solid and hollow hexagonal close-packed melanosomes. (*a*) Predicted gap–midgap ratios versus openness for solid and hollow melanosomes (black and grey lines, respectively). Openness is defined as the proportional amount of keratin between solid melanosomes (w^*) and air within hollow melanosomes (l^*); the gap–midgap ratio is the width of a photonic band gap divided by the frequency in the middle of the gap (see electronic supplementary material, appendix S4 for details). Additional lines for hollow melanosomes show effects of increasing space between melanosomes from the observed close packing (dark grey, close-packed $w^* = 0$; medium grey, $w^* = 0.1$; light grey, $w^* = 0.2$). Points are gap–midgap ratios calculated from morphological data for solid and hollow melanosomes (filled and open circles, respectively; see electronic supplementary material, table S1). Schematic diagram shows morphology as a function of openness for each melanosome type. (*b*) Empirical colourspace showing standardized saturation (peak width divided by hue) versus hue for solid and hollow melanosomes (closed and open circles, respectively). Reflectance peak width was standardized for comparison with modelled results in (*a*) following [23]. Note difference in *y*-axis scale. Polygons are convex hulls delimiting colourspace occupied by each melanosome type (solid: continuous line, hollow: dashed line).

Increased morphological complexity can remove constraints on evolution [3]. Our data show that hollow melanosomes increase the optical complexity of iridescent nanostructures in birds by adding additional interfaces for interaction with light. Because the openness of close-packed hollow melanosomes is determined not only by the spacing between but also by the amount of air within melanosomes, these structures can produce bright colours even when close-packed (figures 3 and

4*b*). In turn, this configuration produces strong nanoscale ordering (figure 1*b,d*) and, in some cases, remarkable colour changes with angle (figure 2*d*). Thus, because close-packed nanostructures are more thermodynamically stable and therefore more likely to form by self-assembly [24], bright nanostructures may evolve more frequently in lineages with hollow melanosomes. Although air can also be introduced by arranging melanosomes in a square lattice [25], this is likely an unstable and limited

configuration (indeed, melanosomes cannot be suspended entirely in air), potentially explaining why it is found less frequently than close-packed configurations [9]. Interestingly, close-packed arrangements are also more mechanically stable than other forms [26], suggesting that they may confer additional tensile properties to feathers.

Although birds have diverse melanosome morphologies and arrangements, and hollow melanosomes are likely one of many innovations that have expanded colourspace, our results may be generalizable to other nanostructures as well. For example, the brilliant colours of hummingbirds (Trochilidae) produced by stacks of hollow platelets [27] would not be possible with solid close-packed platelets, as this configuration would effectively act as a thick layer of bulk melanin and absorb rather than coherently scatter light.

Our morphological and spectral results confirmed that hexagonal arrangements of hollow melanosomes in feather barbules act as two-dimensional PCs. First, TEM and SEM showed that melanosomes are air-filled and cylindrical (see figure 1 and electronic supplementary material, figure S2). Second, spectral results revealed that primary and secondary reflectance peaks for TE-polarized light were much broader and taller in both species than for TM-polarized light (figure 2a,b), matching the photonic band structure prediction (see electronic supplementary material, figure S5) and agreeing with theoretical results for similar photonic structures containing air [15]. Third, the empirical band structures computed from the specular reflectance curves matched the theoretical band structure fairly well (see electronic supplementary material, figure S6), and the colour shift observed in wild turkeys is possible only with a two-dimensional nanostructure (or three-dimensional, but this is clearly not the case here, see electronic supplementary material, figure S2) and was well explained by our optical model (figure 3b). Our modelling results rely on optical parameters (refractive index, absorption) that have never been empirically measured for avian melanin [28]. Some of the discrepancies between theoretical and empirical results (figure 3) may be attributable, in part, to differences between assumed and actual values, and measurement of such values is critically required. Nevertheless, these discrepancies in hue are well within the range, or lower than other previous reports in the literature (e.g. up to 90 nm in [29]), and our results strongly support our hypothesized colour mechanism.

We did not observe an abrupt shift in colour for starlings as we observed in the turkey; rather, the primary peak remained visible over a wide range of observation angles (figure 2c). This may be because starling barbules are strongly curved, whereas turkey barbules are almost flat (figure 1b,d, right insets). Barbule curvature influences the orientation of melanosome layers with respect to the observer and varies along the barbule surface. Thus, the observed colour is averaged over

many crystal orientations [30] and is therefore diffuse as previously described in fruit doves [31] and peacocks [32]. Similar macrostructural features may explain why, contrary to theoretical predictions, feathers with hollow melanosomes were not uniformly brighter than those with solid melanosomes.

Abrupt colour changes have recently been described in a bird-of-paradise (*Parotia lawesii*) [33] as a result of boomerang-shaped barbules. However, wild turkeys had flat barbules and their colour change with tilt is more comparable with that of three-dimensional PCs in weevils [30] and butterflies [34]. Continuous changes in colour with viewing angle (iridescence *sensu* Newton [35]) are common in birds [10,32,36] but, to the best of our knowledge, this is the first description of discrete colour change resulting solely from nanostructure tilt (spectral iridescence, *sensu* [37]). Compared with continuous (graded) signals, discrete signals that vary abruptly may convey different aspects of individual quality or serve a signalling role themselves. Future studies should investigate potential sources of inter-individual variation in this dynamic trait (e.g. variation in nanoscale ordering of melanosomes), as well as the role of such discrete colour shifts in mating displays.

Birds have highly diverse plumage colours that likely evolve by intersexual selection [5], yet, the observed distribution of colours is uneven and restricted relative to what birds can perceive [38], possibly owing to constraints on mechanisms of colour production [39]. Hollow melanosomes may release some of this constraint by providing additional interfaces for light scattering and allowing different colours to be produced by the same colour-producing morphologies. This finding provides a potential mechanistic explanation for broad macroevolutionary patterns such as increased colour diversification in lineages with hollow melanosomes [40], and may also provide inspiration for mechanically stable PC fibres.

References

1. Podos J. 2001 Correlated evolution of morphology and vocal signal structure in Darwin's finches. *Nature* **409**, 185–188. (doi:10.1038/35051570)

2. Mitchison GJ. 1977 Phyllotaxis and the fibonacci series. *Science* **196**, 270–275. (doi:10.1126/science.196.4287.270)

3. Wainwright PC. 2007 Functional versus morphological diversity in macroevolution. *Annu. Rev. Ecol. Evol. Syst.* **38**, 381–401. (doi:10.1146/annurev.ecolsys.38.091206.095706)

4. Grether GF, Kolluru GR, Nersissian K. 2004 Individual colour patches as multicomponent signals. *Biol. Rev.*

Camb. Philos. Soc. **79**, 583–610. (doi:10.1017/S1464793103006390)

5. Andersson M. 1994 *Sexual selection*. Princeton, NJ: Princeton University Press.

6. Hill GE. 2006 Female mate choice for ornamental coloration. In *Bird coloration:* vol. II (eds KJ Mcgraw,

GE Hill), pp. 137–200. Cambridge, MA: Harvard University Press.

7. Prum RO. 2006 Anatomy, physics, and evolution of structural colors. In *Bird coloration,* vol. I (eds KJ Mcgraw, GE Hill), pp. 295–353. Cambridge, MA: Harvard University Press.

8. Maia R, Macedo RHF, Shawkey MD. 2012 Nanostructural self-assembly of iridescent feather barbules through depletion attraction of melanosomes during keratinization. *J. R. Soc. Interface* **9**, 734–743. (doi:10.1098/rsif.2011.0456)

9. Durrer H. 1977 Schillerfarben der vogelfeder als evolutionsproblem. *Denkschr. Schweiz. Naturf. Ges.* **91**, 1–127.

10. Eliason CM, Shawkey MD. 2012 A photonic heterostructure produces diverse iridescent colours in duck wing patches. *J. R. Soc. Interface* **9**, 2279–2289. (doi:10.1098/rsif.2012.0118)

11. Torquato S, Truskett TM, Debenedetti PG. 2000 Is random close packing of spheres well defined? *Phys. Rev. Lett.* **84**, 2064–2067. (doi:10.1103/PhysRevLett.84.2064)

12. Vigneron JP, Colomer J-F, Rassart M, Ingram A, Lousse V. 2006 Structural origin of the colored reflections from the black-billed magpie feathers. *Phys. Rev. E* **73**, 021914. (doi:10.1103/PhysRevE.73.021914)

13. Dyck J. 1976 Structural colours. *Proc. Int. Ornithol. Congr.* **16**, 426–437.

14. Shawkey MD, Estes A, Siefferman LM, Hill GE. 2003 Nanostructure predicts intraspecific variation in ultraviolet–blue plumage colour. *Proc. R. Soc. Lond. B* **270**, 1455–1460. (doi:10.1098/rspb.2003.2390)

15. Joannopoulos JD, Johnson SG, Winn JN, Meade RD. 2008 *Photonic crystals: molding the flow of light.* Princeton, NJ: Princeton university press.

16. Berthier S. 2006 *Iridescences: the physical colors of insects.* New York, NY: Springer.

17. Montgomerie R. 2006 Analyzing colors. In *Bird coloration,* vol. I (eds KJ Mcgraw, GE Hill), pp. 90–147. Cambridge, MA: Harvard University Press.

18. Maia R, Eliason CM, Bitton P-P, Doucet SM, Shawkey MD. 2013 pavo: an R package for the analysis, visualization and organization of spectral data. *Methods Ecol. Evol.* (doi:10.1111/2041-210X.12069)

19. Johnson S, Joannopoulos J. 2001 Block-iterative frequency-domain methods for Maxwell's equations in a planewave basis. *Opt. Express* **8**, 173–190. (doi:10.1364/OE.8.000173)

20. Oskooi A, Roundy D, Ibanescu M, Bermel P, Joannopoulos J, Johnson S. 2010 MEEP: a flexible free-software package for electromagnetic simulations by the FDTD method. *Comput. Phys. Commun.* **181**, 687–702. (doi:10.1016/j.cpc.2009.11.008)

21. Ohring M. 1992 *The materials science of thin films.* San Diego, CA: Academic Press.

22. Noh H. 2009 Optical properties of nanostructures: from random to periodic. **70**, 1–133.

23. Thijssen M, Sprik R, Wijnhoven J, Megens M, Narayanan T, Lagendijk A, Vos W. 1999 Inhibited light propagation and broadband reflection in photonic air-sphere crystals. *Phys. Rev. Lett.* **83**, 2730–2733. (doi:10.1103/PhysRevLett.83.2730)

24. Zhang J, Li Y, Zhang X, Yang B. 2010 Colloidal self-assembly meets nanofabrication: from two-dimensional colloidal crystals to nanostructure arrays. *Adv. Mater.* **22**, 4249–4269. (doi:10.1002/adma.201000755)

25. Zi J, Yu X, Li Y, Hu X, Xu C, Wang X, Liu X, Fu R. 2003 Coloration strategies in peacock feathers. *Proc. Natl Acad. Sci. USA* **100**, 12 576–12 578. (doi:10.1073/pnas.2133313100)

26. Staab GH. 1999 *Laminar composites.* Woburn, MA: Butterworth-Heinemann.

27. Greenewalt C, Brandt W, Friel D. 1960 Iridescent colors of hummingbird feathers. *J. Opt. Soc. Am.* **50**, 1005–1013. (doi:10.1364/JOSA.50.001005)

28. Shawkey MD, Morehouse N, Vukusic P. 2009 A protean palette: colour materials and mixing in birds and butterflies. *J. R. Soc. Interface* **6**, S221–S231. (doi:10.1098/rsif.2008.0459.focus)

29. Saranathan V, Forster JD, Noh H, Liew SF, Mochrie SGJ, Cao H, Dufresne ER, Prum RO. 2012 Structure and optical function of amorphous photonic nanostructures from avian feather barbs: a comparative small angle x-ray scattering (SAXS) analysis of 230 bird species. *J. R. Soc. Interface* **9**, 2563–2580. (doi:10.1098/rsif.2012.0191)

30. Wilts BD, Michielsen K, Kuipers J, De Raedt H, Stavenga DG. 2012 Brilliant camouflage: photonic crystals in the diamond weevil, *Entimus imperialis. Proc. R. Soc. B* **279**, 2524–2530. (doi:10.1098/rspb.2011.2651)

31. Dyck J. 1987 Structure and light reflection of green feathers of fruit doves (*Ptilinopus* spp.) and an imperial pigeon (*Ducula concinna*). *Biol. Skr. K. Dan. Vidensk. Selsk.* **30**, 2–43.

32. Yoshioka S, Kinoshita S. 2002 Effect of macroscopic structure in iridescent color of the peacock feathers. *Forma* **17**, 169–181.

33. Stavenga DG, Leertouwer HL, Marshall NJ, Osorio D. 2011 Dramatic colour changes in a bird of paradise caused by uniquely structured breast feather barbules. *Proc. R. Soc. B* **278**, 2098–2104. (doi:10.1098/rspb.2010.2293)

34. Saranathan V, Osuji CO, Mochrie SGJ, Noh H, Narayanan S, Sandy A, Dufresne ER, Prum RO. 2010 Structure, function, and self-assembly of single network gyroid (I4132) photonic crystals in butterfly wing scales. *Proc. Natl Acad. Sci. USA* **107**, 11 676–11 681. (doi:10.1073/pnas.0909616107)

35. Newton I. 1704 *Opticks.* Mineola, NY: Dover Publications.

36. Osorio D, Ham A. 2002 Spectral reflectance and directional properties of structural coloration in bird plumage. *J. Exp. Biol.* **205**, 2017–2027.

37. Seago AE, Brady P, Vigneron JP, Schultz TD. 2009 Gold bugs and beyond: a review of iridescence and structural colour mechanisms in beetles (Coleoptera). *J. R. Soc. Interface* **6**, S165–S184. (doi:10.1098/rsif.2008.0354.focus)

38. Stoddard MC, Prum RO. 2011 How colorful are birds? Evolution of the avian plumage color gamut. *Behav. Ecol.* **22**, 1042–1052. (doi:10.1093/beheco/arr088)

39. Prum ROR, Lafountain AMA, Berro JJ, Stoddard MCM, Frank HAH. 2012 Molecular diversity, metabolic transformation, and evolution of carotenoid feather pigments in cotingas (Aves: Cotingidae). *J. Comp. Physiol. B* **182**, 1095–1116. (doi:10.1007/s00360-012-0677-4)

40. Maia R, Rubenstein DR, Shawkey MD. 2013 Key ornamental innovations facilitate diversification in an avian radiation. *Proc. Natl Acad. Sci. USA* **110**, 10 687–10 692. (doi:10.1073/pnas.1220784110)